Ferroelectrics, 1993, Vol. 143, pp. 99–107
Reprints available directly from the publisher
Photocopying permitted by license only

EPR STUDIES OF PHASE TRANSITIONS AND INCOMMENSURATE STATES IN $3d^n$-IONS DOPED $MgSiF_6 \cdot 6H_2O$ CRYSTALS

A. M. ZIATDINOV and V. G. KURYAVYI

Institute of Chemistry, Far East Branch of the Russian Academy of Sciences, 690022 Vladivostok, Russia

(Received June 22, 1992)

Electron paramagnetic resonance (EPR) of Mn^{2+}, Ni^{2+}, and Cu^{2+} in magnesium fluosilicate hexahydrate ($MgSiF_6 \cdot 6H_2O$) crystals has been studied at *X*- and *Q*-band frequency in the temperature interval 77 ÷ 400 K. At cooling of crystals with natural abundance of $3d^n$-ions, at $T_{i1} = 370 \mp 0.5$ K, $T_{i2} = 344 \mp 0.5$ K, $T_c = 296 \mp 0.3$ K structural phase transitions of the second and the first (the latter two) order were observed. The transition at T_{i1} is of paraphase-incommensurate phase type, and up to T_{i2} the form of Ni^{2+} and Mn^{2+} EPR lines can be well described in the limit of plane-wave modulation of lattice displacements. At $T \rightarrow T_{i1}$, the amplitude of the trigonal modulation decreases according to the power law with a critical exponent $\beta = 0.35 \mp 0.02$. Below T_{i2} up to T_c the Mn^{2+} line shape was analyzed using the structural soliton model. At $T \rightarrow T_c$, a succession of step-wise changes in the slope of Mn^{2+} line shape parameter curves which are less significant than those at T_{i2} is observed. These step-wise discontinuities in all samples occur at practically the same amounts of line shape parameters. The Cu^{2+} ions affect T_{i1} to the greatest extent if compared to other investigated admixture ions. At T_c crystals undergo an improper ferroelastic first-order phase transition with the unit cell doublet.

Keywords: EPR, magnesium fluosilicate hexahydrate, improper ferroelastic, incommensurate phase, structural solitons

I. INTRODUCTION

Magnesium fluosilicate hexahydrate (MFSH) belongs to isomorphous compounds of the type $ABF_6 \cdot 6H_2O$ (where *A* and *B* are divalent and fourvalent metals, respectively) in which two complex ions $A(H_2O)_6^{2+}$ and BF_6^{2-} form a distorted CsCl-type lattice. Following early crystallographic studies,[1–3] all of these compounds were thought to have the same rhombohedral structure with space group $R\bar{3}$. In this structure, the A^{2+} ions occupy sites of C_{3i} point symmetry in the centre of a trigonally distorted octahedron of water molecules. Recently, there appeared a number of papers, which show a considerable variety of crystalline structures for these compounds.[4–9] A number of compounds are characterized by an improper ferroelastic phase transition from a rhombohedral modification to a low-temperature monoclinic phase.[4,5,10–13] The latter is stable at low temperatures, but there is a diversity of structures observed in the high-temperature region. Jehanno and Varret,[7] Chevrier and Jehanno,[8] and Chevrier *et al.*[9] have carried out thorough and detailed studies of the high-temperature phases of Fe^{2+} and Mg^{2+} compounds. In all cases, the high-temperature structure appears to be closely related to that of the low temperature phase. The structural model proposed for MFSH above 300 K (space group $P\bar{3}$)[8] accounts for the observed extra reflections and corresponds

to an integer periodic antiphase built on the monoclinic ordered cell of the low-temperature form ($P2_1/c$).

In this paper we present EPR investigations with temperature of MFSH crystals containing i) natural abundance of $3d^n$-ions ($\lesssim 10^{-3}$ at.%), ii) $\simeq$1 and 10 at.% Mn^{2+}, iii) $\simeq$5 and 10 at.% Ni^{2+}, iv) $\simeq$1 and 10 at.% Cu^{2+} and of v) γ-irradiated undoped MFSH crystals with emphasis on features related to the discovered structure modulated phases of crystals realized at high temperatures ($T > 296$ K).

II. EXPERIMENTAL PROCEDURE

The EPR measurements were carried out using X- and Q-band spectrometers in three mutually perpendicular crystal planes. The studies were performed in the temperature range 77 ÷ 400 K in both frequency ranges. Copper-constantan thermocouples were used to monitor temperatures above that of liquid nitrogen with one junction attached to the outside of the waveguide close to the sample. The accuracy in measuring the temperature was $\simeq$0.3°K.

Single crystals of MFSH doped with $3d^n$-ions were prepared from aqueous solutions at room temperature. The fluosilicates were purchased commercially. The trigonal $\bar{c}$-axes in most of the samples in these experiments were readily identified by inspection and then they were identified as the [III] direction in cubic coordinates.

The MFSH crystals with natural abundance of Mn^{2+} were irradiated by γ-rays at room temperature. The density of the stable radicals formed by γ-irradiation in the crystals, with $g = 2.0028 \mp 0.0003$, is considered to be proportional to the amount of integral dose of γ-rays and was used to control the radiation dose. In order to avoid errors due to the difference of samples, the same sample was irradiated repeatedly after first irradiation.

III. EXPERIMENTAL RESULTS

The EPR investigations of MFSH crystals containing natural abundance of $3d^n$-ions and $\simeq$1 at.% Mn^{2+} show (see Figure 1) that at cooling at $T_{i1} = 370 \mp 0.5$ K, $T_{i2} = 344 \mp 0.5$ K, $T_c = 296 \mp 0.3$ K they undergo structural phase transformations of the second and the first (the latter two) order. Thus MFSH crystals have 4 structural modifications which are further designated as I, II, III and IV with decreasing temperature.

In phase I ($T > T_{i1}$) at a constant external magnetic field ($\bar{H}$) parallel to $\bar{c}$-axis the Mn^{2+} ($3d^5$, $S = 5/2$, $I = 5/2$) EPR spectrum consists of 6 × 5 hyper-fine structure (HFS) lines with Lorentzian line shapes corresponding to one type of Mn^{2+} axial centres with the axial symmetry axis parallel to the $\bar{c}$-axis in the sites of Mg^{2+} substitution. It is described by a standard axial spin Hamiltonian with parameters:

$$g = 2{,}0009 \mp 0.0003, \qquad D = (-258 \mp 1)\cdot 10^{-4}\ \mathrm{cm}^{-1},$$

$$a = (8 \mp 0.5)\cdot 10^{-4}\ \mathrm{cm}^{-1}, \qquad A_\perp \cong A_\parallel = (-90 \mp 0.5)\cdot 10^{-4}\ \mathrm{cm}^{-1}.$$

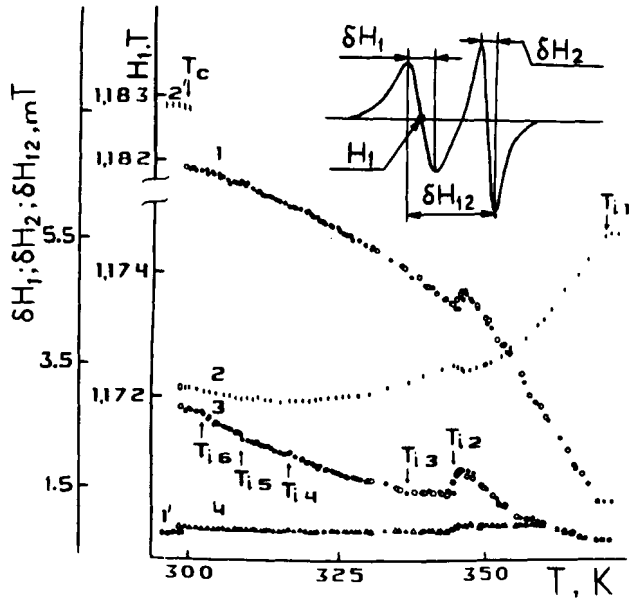

FIGURE 1 Temperature dependences of the parameters of the Mn^{2+} (~1%) EPR low field HFS line in MFSH crystals at Q-band and $\bar{H} \| \bar{c}$. 1—δH_{12}, 2—H_1, 3—δH_1, 4—δH_2; 1′ and 2′ are the position and width of the low field line lower T_c, respectively. The black and white points refer to parameters at heating and cooling of the crystals, respectively. Definitions of the all studied line field parameters are presented too.

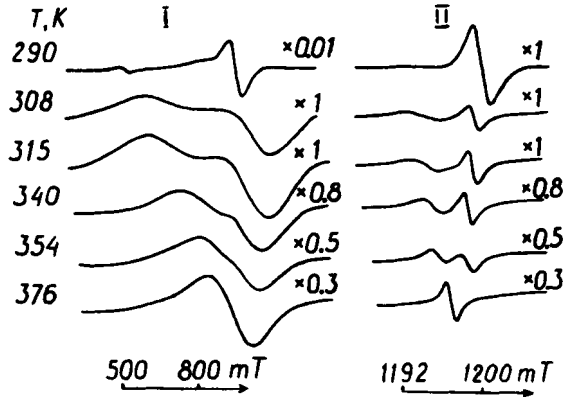

FIGURE 2 Temperature evolution of the Ni^{2+} (~5%) EPR line shape in MFSH crystals at Q-band and $\bar{H} \| \bar{c}$ (I). At 290 K (in ferroelastic phase), the low field line with small intensity corresponds to the transition between the $M_S = \mp 1$ doublet. For comparision, the evolution of the Mn^{2+} (natural abundance) EPR low field HFS line shape of the same crystal is shown (II).

In this phase, the Ni^{2+} ($3d^8$, $S = 1$) EPR spectrum at Q-band and at $\bar{H} \| \bar{c}$ consists of a single broad fine structure (FS) line (see Figure 2) corresponding to the transition within the electron spin levels with $M_S = 0$ and $|M_S| = 1$. As in the case of Mn^{2+}, the Ni^{2+} EPR spectrum in phase I corresponds to one type of axial centres with the axial axis parallel to the $\bar{c}$-axis in the sites of Mg^{2+} substitution. It is described by an appropriate axial spin Hamiltonian with parameters:

$$g = 2.25 \mp 0.02, \qquad |D| = (1.9 \mp 0.1) \cdot \text{cm}^{-1}.$$

At all temperatures above T_c, the single Cu^{2+} EPR line is slightly anisotropic with parameters:

$$g_{\parallel} = 2.23 \mp 0.01, \qquad g_{\perp} = 2.25 \mp 0.01,$$

where the axial axis is along the $\bar{c}$-axis of the crystal. This anisotropy has been shown to result from the trigonal component of the crystalline field.[14] In phase I, the peak-to-peak widths were $\delta H_{\parallel} \approx 50$ mT and $\delta H_{\perp} \approx 40$ mT.

These spectra of $3d^n$-ions are characteristic of the rhombohedral phase ($R\bar{3}$) in crystals of the type studied.[10,14]

The transition at T_{i1} is accompanied by a smooth inhomogeneous broadening of Mn^{2+} and Ni^{2+} EPR lines. Below T_{i1}, these lines are gradually transformed into a two-peak spectrum except for the slightly asymmetric HFS lines of the central Mn^{2+} group (see Figures 1 and 2). It should be noted that up to T_c, the spectrum

TABLE I

The phase transition temperatures in MFSH crystals at cooling (cool.) and heating (heat.) of samples versus nature and concentration of defects

Nature of defects	Concentration (at.%)	$(T_c \mp 0.3)$, K		T_{i2}, K		T_{i1}, K
		heat.	cool.	heat.	cool.	
Mn^{2+}	$\lesssim 10^{-3}$	299.4	296.5	343.5 ∓ 0.5	342.5 ∓ 0.5	370 ∓ 0.5
Mn^{2+}	≈1	299.4	296.5	343.5 ∓ 0.5	342.5 ∓ 0.5	370 ∓ 0.5
Mn^{2+}	≈10	296.5	295.1	344.5 ∓ 1	344.3 ∓ 1	368 ∓ 1
Ni^{2+}	≈5	300.3	297.2	341.5 ∓ 1	341.0 ∓ 1	368 ∓ 1
Ni^{2+}	≈10	301.2	300.1	339.0 ∓ 2	338.8 ∓ 2	367 ∓ 1
Cu^{2+}	≈1	299.2	296.7	339.5 ∓ 1	339.2 ∓ 1	360 ∓ 1
Cu^{2+}	≈10	299.0	296.8	344.5 ∓ 2	344.3 ∓ 2	359 ∓ 2
$\lesssim 10^{-3}$ at.% Mn^{2+}, γ-irradiated; dose ~ 5 Mrad.		298.1	296.0	341.7 ∓ 0.5	341.0 ∓ 0.5	366 ∓ 0.5
$\lesssim 10^{-3}$ at.% Mn^{2+}, γ-irradiated; dose ~ 10 Mrad.		298.8	296.6	341.0 ∓ 0.5	340.0 ∓ 0.5	364 ∓ 0.5

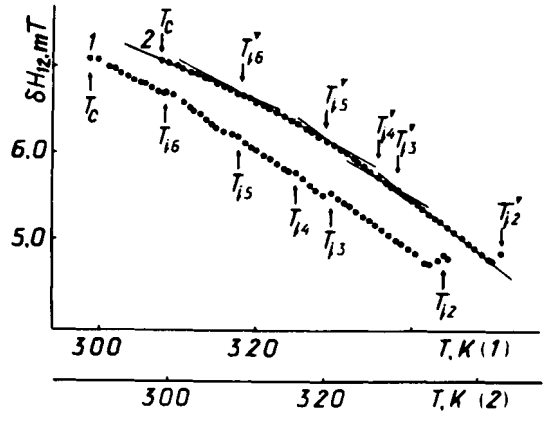

FIGURE 3 Temperature dependence of the value of the Mn^{2+} (~1%) EPR low field HFS line splitting δH_{12} in MFSH crystals between T_c and T_{i2} for two different samples (1 and 2) at X-band and $\bar{H} \| \bar{c}$. The temperatures of the step-wise changes of the slope of the curve $\delta H_{12}(T)$ are denoted as T_{in} and T'_{in} ($n = 2 \div 6$) for samples 1 and 2, respectively.

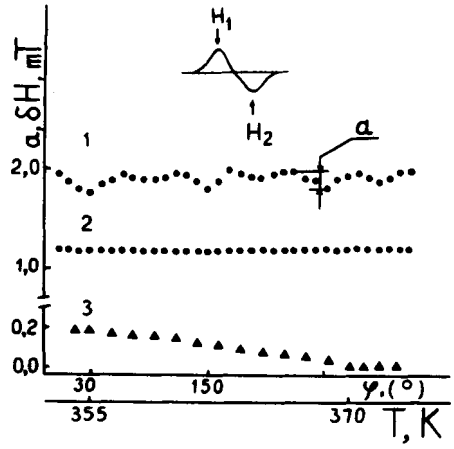

FIGURE 4 Angular dependences of the value of Mn^{2+} ($\simeq$1%) EPR low field HFS line splitting $\delta H_{12} = |H_1 - H_2|$ in MFSH crystals at rotating of the sample around the $\tilde{c}$-axis (along the θ), which makes the angle $\theta = 50°$ with $\tilde{H}$ at 358 K (1) and 375 K (2) and temperature dependence of $a = |\delta H_{12(\max.)} - \delta H_{12(\min.)}|$ (3) at X-band.

axial axes are preserved along $\tilde{c}$-axis. The T_{i1} value is independent of the direction of the temperature changes, the frequency of the microwave field and the value of HFS or FS line splittings. Basing on these data, T_{i1} may be considered as the actual temperature of the second-order phase transition. At T_{i2}, all spectrum and line shape parameters of Mn^{2+} and Ni^{2+} undergo small, but sharp close to step-wise changes with the temperature hysteresis of $\simeq 1°$ (see Figure 1 and Table I). At $T \to T_c$, a succession of step-wise changes in the slope of Mn^{2+} line shape parameter curves which are less significant than those at T_{i2} is observed (see Figures 1 and 3). The temperatures of these step-wise discontinuities T_{in} ($n = 3 \div 6$) vary from sample to sample within the limit of $\sim 4°$, but whatever they occurs at practically the same amounts of line shape parameters (see Figure 3). Having larger FS line width and, as a consequence, a larger value of experimental error, Ni^{2+} parameters do not fix these transitions. At rotating the crystals around the $\tilde{c}$-axis (along the φ angle), which makes a certain angle $\theta \neq 0°, 90°$ with $\tilde{H}$, Mn^{2+} HFS lines do undergo complicated changes which are repeated every 120° (see Figure 4). The maximum amplitude of such changes increases at $T \to T_c$.

The improper ferroelastic phase transition occurs at cooling of the undoped samples at 296 ∓ 0.3 K. The value of the temperature hysteresis of transition is $\simeq 3°$. In phase IV, the EPR spectra of Mn^{2+} and Ni^{2+} correspond to six space-inequivalent rhombohedral centres, two from each orientational domain. The principal axis of a single centre for both kinds of ions and the crystal trigonal axis are rotated by $(8 \mp 2)°$. The angular dependence of a single magnetic centre spectrum for both kinds of ions is in good agreement with the spin Hamiltonian of a rhombohedral symmetry with the following parameters (290 K):

Mn^{2+}:

$$g = 2.0010 \mp 0.0005, \qquad D = (-275 \mp 2) \cdot 10^{-4}\ \text{cm}^{-1},$$

$$|E| = (30 \mp 5) \cdot 10^{-4}\ \text{cm}^{-1}, \qquad a = (8 \mp 2) \cdot 10^{-4}\ \text{cm}^{-1},$$

$$A_\perp \cong A_\parallel = (-92 \mp 1) \cdot 10^{-4}\ \text{cm}^{-1}.$$

Ni^{2+}:

$$g = 2.25 \mp 0.01, \qquad D = (2.20 \mp 0.05)\cdot cm^{-1},$$
$$|E| = (0.23 \mp 0.05)\cdot cm^{-1}.$$

The Cu^{2+} EPR spectrum in a ferroelastic phase similar to Mn^{2+} and Ni^{2+} spectra corresponds to six crystallographically nonequivalent positions of ions, two from each orientational domain. However, in this case, in spite of the monoclinic space symmetry of the crystalline phase ($P2_1/c$)[5] the spectrum of a single magnetic centre has an axial symmetry. The six axially symmetric sets of Cu^{2+} lines have their axial axes parallel to the three tetragonal axes of two cubes, which were rotated by approximately (38 ∓ 2)° with respect to each other about a common [III] axis (the crystal $\bar{c}$-axis). That is, the axial axes of admixture ions and the crystal $\bar{c}$-axis are rotated by (53 ∓ 2)°. The measured g-values were (77 K):

$$g_{\parallel} = 2.40 \mp 0.02, \qquad g_{\perp} = 2.12 \mp 0.02.$$

Precise estimates of the HFS splittings could not be made up to 77 K.

The above type of the Mn^{2+} and Ni^{2+} EPR spectra is characteristic for the monoclinic phase in studied crystals.[10-14] All pecularities of Cu^{2+} spectrum in the monoclinic phase of MFSH crystals may be explained in terms of Jahn-Teller effect.[14-15]

In Table I the experimental values of the transition temperatures in MFSH crystals containing different magnetic ions (defects) and in γ-irradiated samples are presented. As can be seen from Table I, all kinds of defects lead to lowering T_{i1}, however, Cu^{2+} ions have maximum influence on this phase transition temperature if compared to other investigated admixture ions. The changes of T_{i2} under the influence of defects are in the limits of its variation in crystals from different syntheses. All defects except Ni^{2+} produce an insignificant influence on T_c.

IV. DISCUSSION

In discovered "intermediate" phases II and III of MFSH crystals, Mn^{2+} EPR lines are not separated into several components with Lorentzian and/or Gaussian line shapes, but on the other hand, have the form temperature and angular dependences characteristic for dielectric crystal incommensurate phases. Therefore, Mn^{2+} EPR line shape and temperature dependence in the above crystalline phases have been interpreted in terms of the model analogous to that of Blinc[16] for the interpretation of magnetic resonance spectra in crystal incommensurate phases. The scheme of calculations is as follows.

The calculations of the Mn^{2+} HFS line shape in phases II and III are carried out in the assumption of the one-dimensional lattice modulation which is given by

$$U(x) = A(x)\cos[\Phi(x) + \Phi_0] = A(x)\cos\alpha(x),$$

where $\alpha(x)$ is the phase of the local modulation in the direction of the one-dimensional modulation x, Φ_0 is the phase shift, $A(x) = A_0 + \delta A(x)$ is the amplitude

of the lattice displacement, assumed at calculations as $\delta A(x) << A_0$. The resonance field of a given paramagnetic centre can be expanded in powers of cos $\alpha(x)$

$$H = H_0 + h_1(x)\cos\alpha(x) + h_2(x)\cos^2\alpha(x) + \ldots,$$

where H_0 indicates the resonance field corresponding to the structure without modulation, parameters h_1 and h_2 are certain functions of x.

The overall line shape $F(H)$ can then be given by analogous to Blinc[16] by the distribution density of the lines

$$f(H) = \frac{\text{const}}{|-\sin\alpha[\Delta^2 + \cos^2 3\alpha]^{1/2} + b\cos\alpha\cdot\cos 3\alpha\cdot\sin 3\alpha|\, dH/dU} \qquad (1)$$

and the Lorentzian line shape of the individual lines $L(H)$, with full width on half height δW, as follows,

$$F(H) = \int L(H - H_r) f(H_r)\, dH_r.$$

In (1) b is the numerical parameter and connected with the soliton density n_s as

$$n_s = \frac{\pi}{2K(1 + \Delta^2)^{-1/2}},$$

where K is the complete elliptic integral of the first kind. The line shape computer simulation results are given in Figure 5 and in Table II.

As shown, the experimental and calculation results are in good agreement. Thus, it is reasonable to admit that the trigonal distortion of an aquacomplex which determines the value of FS parameter of Mn^{2+} and Ni^{2+} EPR spectra are modulated in phases II and III. It should be noted that earlier the EPR of Ni^{2+} in incommensurate phases of crystals was not observed, and the observed two-peak splitting

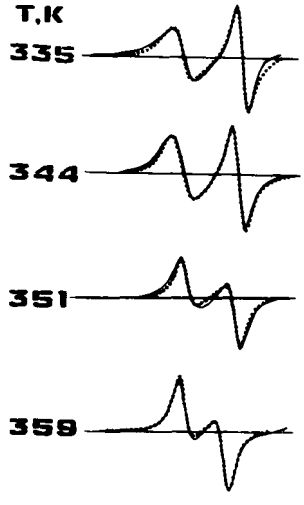

FIGURE 5 Comparison between the experimental (solid line) and the simulated (pointed line) Mn^{2+} ($\simeq$1%) EPR low field HFS line shapes in MFSH crystals at Q-band and $\vec{H}\|\vec{c}$. The simulated line shapes were obtained using the corresponding values of the modulation parameters from Table II.

TABLE II

Values of the modulation parameters, obtained by the fitting between the experimental and the simulated Mn^{2+} (≈1%) EPR low field HFS line shapes in MFSH crystals (see Figure 5)

T, K	h_1, mT	h_2, mT	δW, mT	b	Φ_0, rad.	n_s
335	−2.4	0.9	0.66	1	0.0	0.35
344	−2.3	0.8	0.66	1	−0.2	0.44
351	−2.1	1.0	0.75	0	—	1
359	−1.6	0.5	0.75	0	—	1

of FS lines of Ni^{2+} in the incommensurate phases of MFSH crystals is the maximum one for crystals investigated by means of EPR.

In modulated phase II up to T_{i2}, the spectrum is well interpreted in the approximation of plane-wave modulation of the lattice displacement (soliton density is equal to 1). However, below T_{i2}, the soliton density is not equal to 1 and decreases at lower temperatures, i.e., in phase III the crystal has the inhomogeneous structure and two types of areas: one with a lattice displacement modulation (solitons), the other without it (domains). The transition between the above two incommensurate states have appreciably different lattice displacement modulation character results from the first-order phase transition. This result is, probably, an experimental evidence for the phase transition model of the incommensurate crystals with the multicomponent order parameter proposed by Bake.[17] According to this model, in crystals with multicomponent order parameter, the first-order phase transition into the phase with only one soliton type does prevent the first-order phase transition into the state represented by all structural soliton types. The assumption that only one-type soliton lattice is present in phase III is not in contrast to the above mentioned X-ray structural data of MFSH crystals at $T > 300$ K.[8]

The study of the angular dependence of Mn^{2+} EPR line shape has given extra information elucidating the motive of crystal structural organization in modulated phases. In fact, the availability of angular dependence on φ for Mn^{2+} line shape in phases II and III allows one to draw a conclusion that in the incommensurate phase the cubic crystalline field axes for different Mn^{2+} ions do not coincide due to the rotation of complex ions around the crystal $\bar{c}$-axis. The above disorientation of the cubic crystalline field axes is, probably, connected with the modulation of the rotation angle of the complex ion around the $\bar{c}$-axis relative to the position in the paraphase.

When $\bar{H} \| \bar{c}$ and, consequently, there is no contribution into the inhomogeneously broadened line shape of Mn^{2+} because of the disorientation of the cubic crystalline field axes, at $T \to T_{i1}$ the modulation parameters h_1 and h_2 are described as a function of temperature:

$$h_1 = 0.39(T_{i1} - T)^{\beta}, \tag{2a}$$

$$h_2 = 0.25(T_{i1} - T)^{2\beta}, \tag{2b}$$

(all in mT) with critical index $\beta = 0.35 \mp 0.02$ (see Figure 6).

As first pointed out by Iizumi *et al.*,[18] the structurally incommensurate phase transition in K_2SeO_4 is driven by a two-fold degenerate soft mode satisfying the Landau-Ginsburg-Wilson Hamiltonian. This Hamiltonian has the same universal

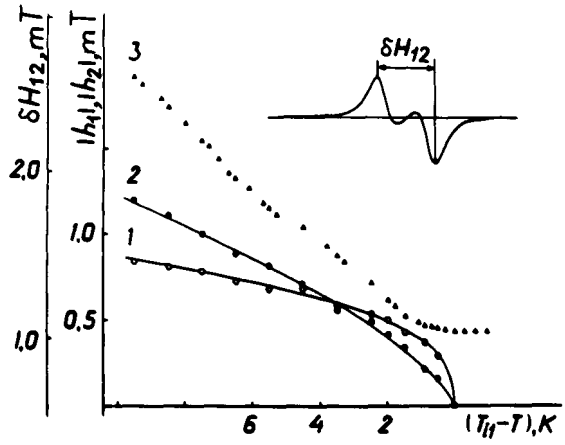

FIGURE 6 Temperature dependences of the value of Mn^{2+} ($\simeq 1\%$) EPR low field HFS line splitting δH_{12} in MFSH crystals at X-band and $\vec{H} \| \vec{c}$ (1) and of modulation parameters h_1 (1) and h_2 (2). The points refer to experimental (δH_{12}) and calculated (h_1, h_2) values of parameters. The solid lines 1 and 2 were obtained from the Equations 2a and 2b, respectively.

features of the 3d − XY model, with the value of the exponent equal to 0.3455 $\mp$ 0.0020, as calculated by Le Guillon and Zinn-Justin.[19] The agreement between the theoretical value of β and that obtained in experiment is very good.

In conclusion, we would like to note that the study of the temperature variation of the width and shape of magnetic ion resonance lines in incommensurate phase and in the vicinity of the phase transition temperatures of the deuterated crystals ($MgSiF_6 \cdot 6D_2O$) will definitely give additional useful information regarding the order parameter of incommensurate phase and the changes in structure motives during the phase transformations, especially at T_{in}. A detailed treatment of such investigation of $MgSiF_6 \cdot 6D_2O$ crystals will be published elsewhere.

REFERENCES

1. O. Hassel, *Z. Phys. Chem.*, **126,** 118 (1927).
2. O. Hassel and J. R. Salvesen, *Z. Phys. Chem.*, **128,** 345 (1927).
3. L. Pauling, *Z. Kristallogr.*, **72,** 482 (1930).
4. E. Kodera, A. Torii, K. Osaki and T. Watanabe, *J. Phys. Soc. Jpn.*, **32,** 863 (1972).
5. S. Syoyama and K. Osaki, *Acta Cryst. Sect. B*, **28,** 2626 (1972).
6. S. Ray, A. Zalkin and D. H. Templton, *Acta Cryst. Sect. B*, **29,** 2741 (1973).
7. G. Jehanno and F. Varret, *Acta Cryst. Sect. A*, **31,** 857 (1975).
8. G. Chevrier and G. Jehanno, *Acta Cryst. Sect. A*, **35,** 912 (1979).
9. G. Chevrier, A. Hardy and G. Jehanno, *Acta Cryst. Sect. A*, **37,** 578 (1981).
10. R. S. Rubins, *Chem. Phys. Lett.*, **28,** 273 (1974).
11. R. S. Rubins, Bobby C. Griffin and Rick Burris, *J. Chem. Phys.*, **64,** 3349 (1976).
12. Yu. V. Yablokov, M. M. Zaripov, A. M. Ziatdinov and R. L. Davidovich, *Chem. Phys. Lett.*, **48,** 443 (1977).
13. A. M. Ziatdinov, V. G. Kuryavyi and R. L. Davidovich, *Sov. Phys.: Solid. State*, **29,** 120 (1987).
14. A. M. Ziatdinov, M. M. Zaripov, Yu. V. Yablokov and R. L. Davidovich, *Phys. Status Sol.*, **B78,** K69 (1976).
15. R. S. Rubins, Lucio N. Tello, D. K. De and D. T. Black, *J. Chem. Phys.*, **81,** 4230 (1984).
16. R. Blinc, P. Prelovsek and R. Kind, *Phys. Rev.*, **B27,** 5401 (1983).
17. P. Bake, Proceedings of the Simposium on Soliton Structure and Dynamics in Condensed Matter, Oxford, 22–29 June, 1978.
18. M. Iizumi, J. D. Axe, G. Shirane and K. Shimaoka, *Phys. Rev. B*, **15,** 4392 (1977).
19. J. C. Le Guillon and J. Zinn-Justin, *Phys. Rev. B*, **21,** 3976 (1980).